

Thermal conductivity of solid argon from molecular dynamics simulations

Konstantin V. Tretiakov^{a)}

The Abdus Salam International Centre for Theoretical Physics (ICTP), Strada Costiera 11, I-34100 Trieste, Italy, and Institute of Molecular Physics, Polish Academy of Sciences, Smoluchowskiego 17/19, 60-179 Poznań, Poland

Sandro Scandolo

The Abdus Salam International Centre for Theoretical Physics (ICTP), Strada Costiera 11, I-34100 Trieste, Italy, and INFN/Democritos National Simulation Center, I-34100 Trieste, Italy

(Received 7 August 2003; accepted 25 November 2003)

The thermal conductivity of solid argon in the classical limit has been calculated by equilibrium molecular dynamic simulations using the Green–Kubo formalism and a Lennard-Jones interatomic potential. Contrary to previous theoretical reports, we find that the computed thermal conductivities are in good agreement with experimental data. The computed values are also in agreement with the high-temperature limit of the three-phonon scattering contribution to the thermal conductivity. We find that finite-size effects are negligible and that phonon lifetimes have two characteristic time scales, so that agreement with kinetic theory is obtained only after appropriate averaging of the calculated phonon lifetimes. © 2004 American Institute of Physics. [DOI: 10.1063/1.1642611]

I. INTRODUCTION

Microscopic models of thermal conduction in condensed systems are increasingly used to predict the heat transfer properties of materials, from semiconductors,¹ to ceramics for high-temperature coatings,² to Earth's mantle minerals.³ We focus here on those systems where thermal conduction is dominated by lattice contributions. This is the case for most insulators, where electronic contributions to heat transfer are hindered by the large excitation gap. Moreover, we restrict our analysis to the high temperature regime, where nuclear quantum effects are negligible and the atomic dynamics can be considered as purely classical.

Various approaches have been proposed to calculate the macroscopic value of the lattice thermal conductivity (λ) at finite temperature, from the atomic dynamics.⁴ In the Green–Kubo approach, λ is calculated from a molecular dynamics (MD) simulation at equilibrium, using the fluctuation-dissipation theorem. In nonequilibrium MD (NEMD) approaches, a stationary heat flux is generated either by direct application of a temperature gradient or by application of an external fictitious field. Either way, calculations of λ generally require large simulation cells and long time scales to converge the statistical sampling. As a consequence, the thermal conductivity of real materials has been calculated so far only for a restricted set of substances, and at best with a semiempirical description of the interatomic interactions.

Argon is, in this context, an interesting exception. Like most other condensed rare gases, the atomic dynamics of argon is in fact described with a very good accuracy by a simple Lennard-Jones (LJ) interatomic pair potential:

$$\phi(r_{ij}) = 4\epsilon \left[\left(\frac{\sigma}{r_{ij}} \right)^{12} - \left(\frac{\sigma}{r_{ij}} \right)^6 \right], \quad (1)$$

where r_{ij} is the distance between atoms i and j . For argon, the values of the parameters ϵ and σ that best reproduce its thermodynamics are $\epsilon/k_B = 119.8$ K and $\sigma = 3.405$ Å, where k_B is the Boltzmann constant.⁴ The simplicity of the interatomic interactions has made argon a benchmark system to test methodological developments and to improve our microscopic understanding of heat transfer in condensed systems. The thermal conductivity of the LJ fluid has been calculated in a number of works.^{5–8} For fluid argon, the comparison of the LJ results with experiment is very satisfactory, the discrepancy being smaller than 10% in a wide temperature range.⁶ However, the thermal conductivity of the LJ *solid* has been studied in much less detail.^{9,10} Comparison of the calculated values with experiments has been attempted only in Ref. 10, where a discrepancy of almost a factor of 2 has been reported. Such a discrepancy is surprising, given the proven reliability of the LJ model in describing the static properties as well as other dynamical properties of solid argon. Similar discrepancies have been found in the calculation of λ at high temperature in other solids,^{3,11,12} which raises the fundamental question of whether the above-described microscopic models are appropriate to provide an accurate description of macroscopic heat transfer in solids.

In this paper we carry out an extensive series of MD simulations of solid argon at zero pressure and at temperatures between 10 and 75 K, and show that the discrepancy of the “LJ” values of λ for solid argon with experiments is less than 20%. This contradicts earlier results¹⁰ and therefore supports the LJ parametrization for argon as well as the validity of the Green–Kubo approach for the calculation of λ in solids. The paper is organized as follows: In Sec. II we describe the Green–Kubo method and present the simulation details. In Sec. III we present the MD results and compare them with previous theoretical and experimental data.^{9,10,13–15} Section IV contains summary and conclusions.

^{a)}Electronic mail: kvt@ictp.trieste.it

II. METHOD

The thermal conductivity λ is defined as the linear coefficient relating the macroscopic heat current \mathbf{J} to the temperature gradient (Fourier's law):

$$\mathbf{J} = -\lambda \cdot \text{grad } T. \quad (2)$$

In this paper we calculate λ using the Green–Kubo formula:⁴

$$\lambda = \frac{1}{3Vk_B T^2} \int_0^\infty \langle \mathbf{j}(0)\mathbf{j}(t) \rangle dt, \quad (3)$$

where V is the volume, T the temperature, and the angular brackets denote the ensemble average, or, in the case of a MD simulation, the average over time. The microscopic heat current is given by

$$\mathbf{j}(t) = \sum_i \mathbf{v}_i \varepsilon_i + \frac{1}{2} \sum_{i,j,i \neq j} \mathbf{r}_{ij} (\mathbf{F}_{ij} \cdot \mathbf{v}_i), \quad (4)$$

where \mathbf{v}_i is the velocity of particle i , \mathbf{F}_{ij} is the force on atom i due to its neighbor j from the pair potential (1). The site energy ε_i is given by

$$\varepsilon_i = \frac{1}{2} m_i |\mathbf{v}_i|^2 + \frac{1}{2} \sum_j \phi(\mathbf{r}_{ij}), \quad (5)$$

where m is the mass of atom.

MD simulations were performed both in the NVT and in the NpT ensemble, to allow for appropriate comparison with experiments, which were in some cases performed under isochoric conditions, and in other cases under isobaric ($p=0$) conditions. Temperature in NVT simulations was controlled via a Nosé–Hoover (NH) thermostat.¹⁶ The fourth-order Kunge–Kutta integration scheme was used to integrate the equations of motion. In order to avoid problems related to unwanted noncanonical fluctuations of the instantaneous temperature in NH thermostatted simulations (the so-called ‘‘Toda demon’’), we follow the prescriptions of Ref. 17. MD simulation in the NpT ensemble was performed using Gear's fourth-order predictor-corrector method to integrate the equation of motion,⁴ and no thermostats. Temperature and volume were rescaled every 5 MD steps.

The integration time step Δt was set to $0.002\tau_{LJ}$ LJ units (the LJ unit of time is $\tau_{LJ} = \sqrt{m \cdot \sigma^2 / \epsilon}$, or 2.16 ps for argon) at low temperatures ($T \leq 50$ K) and $0.005\tau_{LJ}$ otherwise. The typical lengths of the runs were equal to 1.1×10^6 MD steps, after equilibration (10^5 MD steps) at low temperatures and 5.5×10^5 MD steps, after equilibration (5×10^4 MD steps) at high temperatures. Longer runs (5×10^6 MD steps) were also performed to check the convergence of the results on simulation time. The LJ pair potential was cut off at a radius of 2.5σ and long-range corrections to the energy were considered.¹⁸

The thermal conductivity was calculated by discretizing the right-hand side of Eq. (3) in MD time steps (Δt) as

$$\lambda = \frac{\Delta t}{3Vk_B T^2} \sum_{m=1}^M \frac{1}{(N-M)} \sum_{n=1}^{N-m} \mathbf{j}(m+n)\mathbf{j}(n), \quad (6)$$

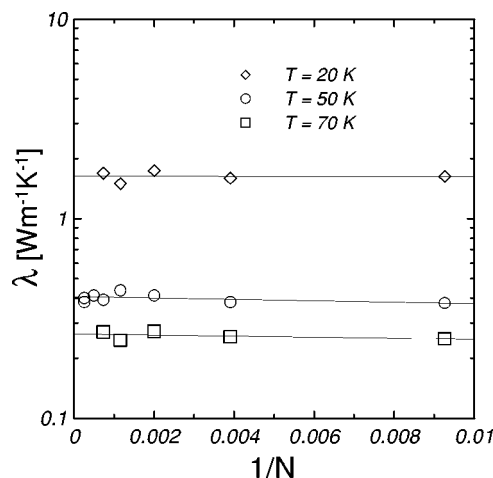


FIG. 1. Calculated thermal conductivity of solid argon as a function $1/N$ where N is the number of particles in the simulation cell. The lines are just a guide to the eye.

where N is the number of MD steps after equilibration, M is the number of steps over which the time average is calculated, and $\mathbf{j}(m+n)$ is the heat current at MD time step $m+n$. M was set to $(1-4) \times 10^4$ at low temperatures and $(4-8) \times 10^3$ at high temperatures, which is considerably smaller than the number of MD steps, in order to ensure good statistical averaging.

Finite-size effects were checked by repeating the simulations with cubic cells containing of $N=4n^3$ particles [solid argon crystallizes in the face-centered cubic (fcc) lattice, with four atoms in the conventional cubic cell] and increasing n from 3 to 10 (which corresponds to $N=108$ to 4000). Periodic boundary conditions were imposed. The behavior of λ with the particle number N for three different temperatures is shown in Fig. 1. It has been argued that larger simulation cells are required to converge the results for the solid at low temperatures,¹⁹ with respect to the fluid. We find that the results for the solid are converged, at 20 K, even with the smallest size considered ($N=108$), which is consistent with the weak size effects found in the study of liquid argon with the Green–Kubo approach.⁶ It is possible that for particle numbers less than $N=108$, size effects with the Green–Kubo method are more important in the solid than in the liquid. However, calculations with $N=108$ are already extremely cheap from a computational point of view, so we consider size effects irrelevant for any practical purpose. Moreover, the size dependence of thermal conductivity has been shown to be minimal also in recent NEMD simulations.²⁰

It is interesting to notice, as already done by others,²¹ that convergence in size is achieved for cell sides that are still much smaller than the phonon mean free path. In fact, we can estimate the phonon mean free path, using kinetic theory, as

$$l = \frac{3\lambda}{C_V c}, \quad (7)$$

where C_V is the specific heat and c is the speed of sound. Using $C_V = 3Nk_B$ and

TABLE I. Comparison of the thermal conductivity of some systems as obtained in the present work (λ , λ^*) and in other theoretical works (λ_{ref} , λ_{ref}^*). Temperatures and densities (T^* and ρ^*) are expressed in reduced units. Thermal conductivities are in reduced units (λ^* , λ_{ref}^*) or W/mK (λ , λ_{ref}).

N	T^*	ρ^*	λ	λ_{ref}
Fluid LJ: Ref. 6				
108	0.73	0.8442	0.124(9)	0.127(3)
108	0.94	0.7149	0.092(7)	0.094(5)
108	1.27	0.6499	0.067(6)	0.070(4)
Fluid LJ: Ref. 7				
N	T^*	ρ^*	λ^*	λ_{ref}^*
108	0.72	0.835	6.6(4)	6.4(3)
108	1.35	0.4	1.75(12)	1.80(9)
108	1.8627	0.9248	10.0(5)	9.9(5)
Solid LJ: Ref. 9				
N	T^*	ρ^*	λ^*	λ_{ref}^*
256	0.55	1.414	352(75)	357(61)
Solid r^{-12} : Ref. 19				
N	T^*	ρ^*	λ^*	λ_{ref}^*
108	0.208	1.414	201(21)	203(10)
108	0.546	1.414	52.6(3.1)	53.2(2.7)
108	1.191	1.414	24.1(1.5)	23.2(1.2)

$$c = \frac{k_B \theta_D}{\hbar k_D}, \tag{8}$$

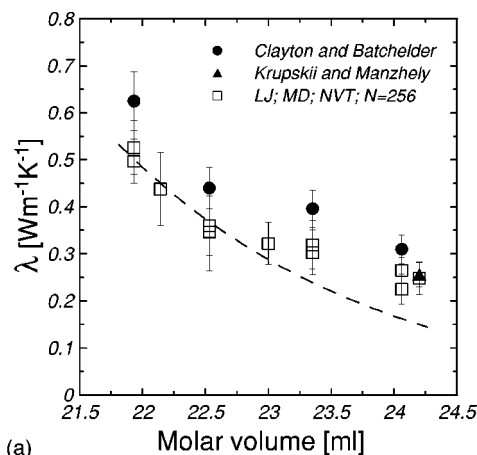
where θ_D is the Debye temperature, \hbar is Planck's constant, and $k_D = \sqrt[3]{6N\pi^2/V}$ is the Debye wave vector, we obtain, for argon at $T=20$ K, a phonon mean free path of $\sim 14\sigma$. On the other hand, Fig. 1 shows that the value of λ is converged even for $N=108$, which corresponds to a cell size of only 4.9σ .

III. RESULTS

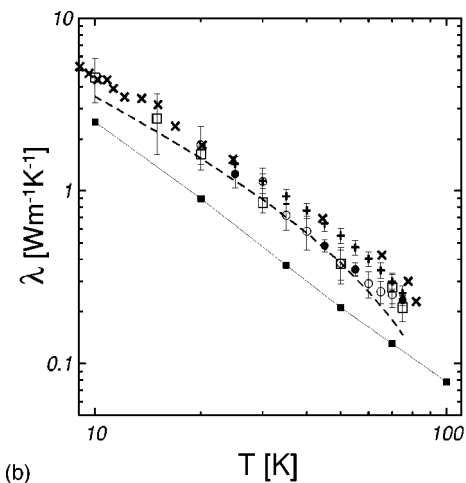
We first compare our results with available theoretical data for fluid argon as well with calculations of the thermal conductivity of the fcc lattice obtained with LJ and inverse-twelfth-power potentials (Table I). The good agreement with previous determinations of λ is a further independent check of the reliability of our calculations.

We now describe the results obtained for solid argon. In Fig. 2(a) we show the dependence of the thermal conductivity of solid argon on the molar volume at 75 K. The simulations were performed in the NVT ensemble. The results are in remarkable agreement with the experimental results of Refs. 13 and 14. Differences between MD simulations and experiments are of the order of 20%, which is smaller than the sum of the MD statistical errors and the experimental error bars.

According to Ref. 22, the high-temperature limit of the thermal conductivity of a cubic crystal with pairwise interactions can be written as



(a)



(b)

FIG. 2. (a) Volume dependence of the thermal conductivity of solid argon at 75 K. The black triangle is the datum of Krupskii and Manzhelii (Ref. 13). The dots are the data of Clayton and Batchelder (Ref. 14). Squares are our results in the NVT ensemble. The broken curve was calculated using Eq. (9). (b) Temperature dependence of the thermal conductivity of solid argon at atmospheric pressure: (+) data from Ref. 13, (x) data from Ref. 15. Black squares are the theoretical results of Kaburaki, Li, and Yip (Ref. 10). Open circles are the results of single runs in the NVT ensemble ($N=108$). Black dots correspond to the average of ten independent runs in the NVT ensemble (notice the reduced error bar with respect to the single runs). Squares are the results of simulations in the NpT ensemble ($N=108$). The broken curve was calculated using Eq. (9).

$$\lambda \sim \frac{C}{aT} \sqrt{\frac{\phi'' (\phi''')^3}{m (\phi''')^2}}, \tag{9}$$

where ϕ'' and ϕ''' are the second and third derivatives, respectively, of the pair interaction potential, m is the atomic mass, a is the lattice spacing of the primitive cubic cell, and C is a dimensionless constant ($C=8.12$ for a LJ fcc solid¹⁵). Even though Eq. (9) was derived under the assumption that only three-phonon terms contribute to λ , it has been argued that the same expression might account in an effective fashion for higher-order phonon scattering processes, if a and the potential terms ϕ'' and ϕ''' are evaluated at the temperature-dependent equilibrium distance between particles,¹⁵ instead of their zero temperature limit. We confirm that such a “quasiharmonic” approximation is indeed an accurate way of accounting for deviations from the T^{-1} law, due to higher-order effects, as can be seen in Fig. 2.

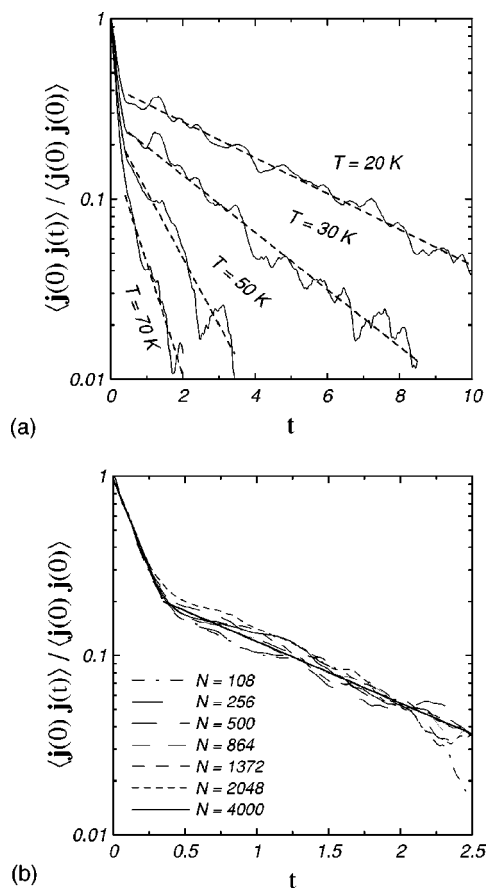


FIG. 3. Heat autocorrelation function: (a) for different temperatures and $N = 108$ particles; (b) at $T = 50$ K and different cell sizes.

In Fig. 2(b) we show the temperature dependence of the thermal conductivity. The agreement with experimental results^{13–15} is remarkable. Notice that points in Fig. 2(b) obtained in the NpT and NVT ensemble agree within the error bars. In Fig. 2(b) we also show the results of an earlier MD simulation of solid argon.¹⁰ Their results disagree with our MD results as well as with experimental data. The methodology used in Ref. 10 was in principle identical to the one used in this work, and the LJ parametrization was also identical to ours. Therefore, we are not in a position to qualify possible sources of discrepancy between the two sets of results.

Typical normalized heat current autocorrelation functions [the integrand of Eq. (3)] are presented in Fig. 3(a) for different temperatures. As expected, the decay of the heat current autocorrelation function is slower at lower temperature, because of the reduced number of scattering processes. It is interesting to notice, however, that none of the curves follows a single exponential decay.^{10,19} This behavior is illustrated in more detail in Fig. 3(b), where the heat flux autocorrelation function at 50 K is displayed for different sizes of the simulation cell. The decay can be modeled with a double-exponential function with a faster component followed by a slower decay. In Table II we report the values of the two characteristic times (τ_1 and τ_2) at different temperatures. We remark that both decays contribute with compa-

TABLE II. Comparison of phonon life times in solid argon. τ_1 and τ_2 are the two components of the heat-current autocorrelation function (see Fig. 3). τ_{av} is the average decay time defined in Eq. (10). τ_{kin} and τ_{expt} are phonon lifetimes extracted from kinetic theory and our data (τ_{kin}) or experimental data (τ_{expt}). All entries are expressed in LJ units (τ_{LJ} see the text for the definition).

$T(K)$	τ_1	τ_2	τ_{av}	τ_{kin}	τ_{expt}
20	0.34	4.27	2.16	2.33	2.18
50	0.23	1.29	0.46	0.58	0.64
70	0.19	0.70	0.28	0.38	0.35

table weight to the integral of Eq. (3). Yet, one can still define an *average* decay time as

$$\tau_{av} = \frac{\int_0^\infty \langle \mathbf{j}(t)\mathbf{j}(0) \rangle dt}{\langle \mathbf{j}(0)\mathbf{j}(0) \rangle} = \frac{\lambda k_B T^2}{3V \langle \mathbf{j}(0)\mathbf{j}(0) \rangle} \quad (10)$$

and compare it to the decay time that can be determined using kinetic theory, $\tau_{kin} = l/c$, with l given by Eq. (7). Using the calculated values for the Debye temperature ($\theta_D = 85.1$ K)¹³ and the calculated values of λ , we find that τ_{kin} is very similar to τ_{av} (see Table II). This suggests that kinetic theory is valid for solid argon, even though with a definition of the phonon lifetime (τ_{av}) which accounts explicitly for the presence of two decay regimes. We notice that τ_{av} compares very well also with the phonon lifetime τ_{expt} extracted, using kinetic theory, from experimental data of λ and θ_D .¹³ On the contrary, estimates of the phonon lifetime based on the long-time decay of the autocorrelation function scattering (τ_2 in Table II) would not be consistent with kinetic theory, as τ_2 is systematically larger than τ_{av} by about a factor of 2.

IV. SUMMARY AND CONCLUSIONS

We have shown that the thermal conductivity of solid argon in the high-temperature (classical) regime determined through accurate MD simulations with a LJ model and the Green–Kubo method is in good agreement with experimental data. This disproves earlier works where a discrepancy of about a factor of 2 was reported.¹⁰

We find that simplified models for the thermal conductivity based on the high-temperature limit of the three-phonon scattering rate^{15,22} reproduce our data rather well, including deviations from the T^{-1} law, if they are evaluated in the quasiharmonic approximation (i.e., at the equilibrium volume for any given temperature).

We confirm that size effects in the determination of the thermal conductivity with the Green–Kubo method are negligible, even for cell sizes much smaller than the phonon mean free path.

In conclusion, our results confirm that the Green–Kubo approach is a very powerful method to calculate the thermal conductivity of crystals at high temperature. Concomitantly with the development of improved interatomic potentials for the description of more complex materials, our results suggest that this approach could soon lead to the prediction of thermal conductivities in materials where experimental data

are difficult to obtain, such as ceramics at high temperatures and minerals at geophysical conditions of pressure and temperature.

ACKNOWLEDGMENTS

We acknowledge useful discussions with R. Car, Y.-G. Yoon, and P. Tangney. The work was partially supported by the Center of Excellence for Magnetic and Molecular Materials for Future Electronics within the EC Contract No. G5MA-CT-2002-04049 and by the National Science Foundation (USA) under the EAR-CSEDI program.

¹J. Dong, O. F. Sankey, and C. W. Myles, *Phys. Rev. Lett.* **86**, 2361 (2001).

²P. K. Schelling and S. R. Phillpot, *J. Am. Ceram. Soc.* **84**, 2997 (2001).

³R. E. Cohen, in *Physics Meets Mineralogy*, edited by H. Aoki, Y. Syono, and R. J. Hemley (Cambridge University Press, Cambridge, 2000), p. 95.

⁴M. P. Allen and D. J. Tildesley, *Computer Simulation of Liquids* (Clarendon, Oxford, 1987).

⁵D. Heyes, *J. Chem. Soc., Faraday Trans. 2*, 1363 (1984).

⁶R. Vogelsang, C. Hoheisel, and G. Ciccotti, *J. Chem. Phys.* **86**, 6371 (1987).

⁷D. Heyes, *Phys. Rev. B* **37**, 5677 (1988).

⁸D. J. Evans, *Phys. Rev. A* **34**, 1449 (1986).

⁹S. Volz, J.-B. Saulnier, M. Lallemand, B. Perrin, Ph. Depondt, and M. Mareschal, *Phys. Rev. B* **54**, 340 (1996).

¹⁰H. Kaburaki, Ju Li, and S. Yip, *Mater. Res. Soc. Symp. Proc.* **538**, 503 (1999).

¹¹Ph. Jund and R. Jullien, *Phys. Rev. B* **59**, 13707 (1999).

¹²Y.-G. Yoon, R. Car, D. J. Srolovitz, and S. Scandolo (unpublished).

¹³I. N. Krupskii and V. G. Manzhelii, *Sov. Phys. JETP* **28**, 1097 (1969).

¹⁴F. Clayton and D. N. Batchelder, *J. Phys. C* **6**, 1213 (1973).

¹⁵D. K. Christensen and G. L. Pollack, *Phys. Rev. B* **12**, 3380 (1975).

¹⁶D. Frenkel and B. Smit, *Understanding Molecular Simulation* (Academic, San Diego, 2002).

¹⁷B. L. Holian, A. F. Voter, and R. Ravelo, *Phys. Rev. E* **52**, 2338 (1995).

¹⁸D. M. Heyes, *The Liquid State Application of Molecular Simulation* (Wiley, Chichester, 1998).

¹⁹A. J. C. Ladd, B. Moran, and W. G. Hoover, *Phys. Rev. B* **34**, 5058 (1986).

²⁰B. L. Holian, *J. Chem. Phys.* **117**, 1173 (2002).

²¹J. Che, T. Cagin, W. Deng, and W. A. Goddard III, *J. Chem. Phys.* **113**, 6888 (2000).

²²G. Leibfried and E. Schlömann, *Nachr. Ges. Wiss. Goettingen, Math.-Phys. Kl.* **2a**, 71 (1954).